Focussed on: Infrared Thermographic Analysis of Materials

Energy dissipation and storage in iron under plastic deformation (experimental study and numerical simulation)

A. Kostina, A. Iziumova, O. Plekhov

Institute of Continuous Media Mechanics of the Ural Branch of the Russian Academy of Sciences, 614013, Ac. Koroleva Street, 1, Perm, Russia
poa@icmm.ru

ABSTRACT. The work is devoted to the experimental and numerical investigation of thermodynamic aspects of the plastic deformation in Armco iron. Dissipation and stored energies was calculated from processed experimental data of the surface temperature obtained by infrared thermography. An original mathematical model describing the process of mesoscopic defects accumulation was used for numerical simulation of the quasistatic loading of iron samples and for calculation of theoretical value of the stored energy. Experimental and modeled values of the stored energy are in a good agreement.

KEYWORDS. Stored energy; Infrared thermography; Mesodefect evolution; Numerical simulation.

INTRODUCTION

The experimental and theoretical study of energy balance in metals under plastic deformation has a long history. The importance of this issue for understanding of nature of irreversible deformation of metals and its transition to fracture was originally shown by J. H. Lambert in 1779 in his statement concerning the energy similarity of mechanical and thermal failure processes of solids. The review of experimental works devoted to the methods of stored energy study in the material under plastic deformation and the peculiarities of this process for different material structures and load conditions is available in [1].

To analyze the thermodynamic characteristics of deformation processes in solids, it is necessary to take into account the fact that the plastic deformation work is converted into two parts: heat energy caused by the movement and annihilation of defects at various structural levels, and hidden (stored) energy of plastic deformation accumulated in the elastic fields of defects. The first part of energy can be detected by different experimental techniques and gives us information about current state of structure evolution.

During the last decades the enhanced ability to detect temperature evolution during mechanical testing leads to a great interest in the application of infrared (IR) thermography to study heat dissipation process caused by defect evolution under plastic deformation in metals. The theoretical and experimental study of this problem can be useful for explanation of many phenomena of mechanics of solids such as cold work evolution, study of damage to fracture transition and crack propagation process, investigation of crack tip closure effect, validation of linear failure mechanics formula to the investigation of fatigue cracks propagation in metals under different loading conditions and so on.

The aforementioned experimental results indicate the importance of further development of methods for investigation of the thermodynamics of the deformation process and develop adequate theoretical models of plastic deformation describing the energy balance in metals under plastic deformation. This work is devoted to investigation of energy dissipation in Armco iron under quasistatic tension. It was shown experimentally [2] that from macroscopic point of view the deformation process of Armco iron can be divided into homogeneous and heterogeneous parts. As a first step of

theoretical consideration of the phenomena we tried to simulate the energy storage process in Armco iron under homogeneous plastic deformation. The simulation was based on the original statistical model of defect evolution and includes the separation of plastic deformation into dissipative and thermodynamic (structural) parts. The nonlinear constitutive equation for structural sensitive parameters allows us to obtain the qualitative agreement between experimental and theoretical results.

MATERIAL AND EXPERIMENTAL CONDITIONS

Experimental study was carried out on the Armco iron specimens. Chemical composition of the examined material is presented in Tab. 1. Fig 1. shows geometry of the specimens.

C	Mn	Si	S	P	Ni	Cr	Mo
0.004	0.04	0.05	0.005	0.005	0.06	0.038	0.01

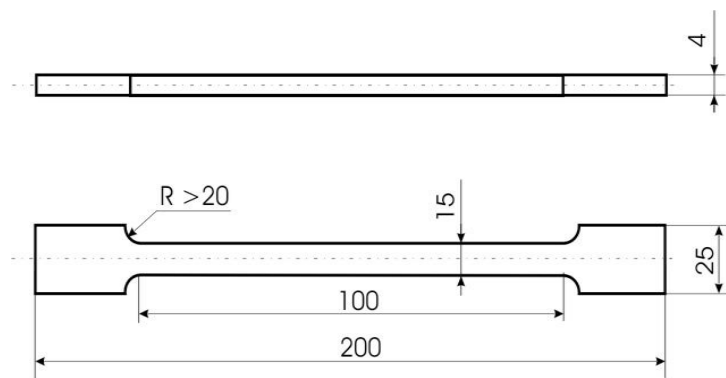Table 1: Armco iron chemical composition (wt%).

Figure 1: Geometry of specimens. All sizes are in millimeters.

After tooling, specimens were annealed in non-oxygen atmosphere with 1073 K temperature during 8 hours. Non-oxygen atmosphere was created by co-annealing of metal and copper samples with developed surface for a better oxidation.
Mechanical test was carried out on servo hydraulic machine INSTRON 8500. Before starting of experiments the surface of the specimens was mechanically polished (at the last stage of the polishing the diamond suspension with a characteristic grit size of 3 microns was used). After polishing the surface was covered of matt black paint. It was done to obtain emissivity of the specimen's surface close to 1 for better conditions of infrared monitoring.
Specimens were loaded in uniaxial stretching mode with strain rate 2·10^{-3} sec^{-1}. Infrared camera CEDIP Jade III was used to record the temperature evolution on the surface during mechanical test. The maximum frame size is 320×256 pixels; the spatial resolution is 10^{-4} meters. The temperature sensitivity is from 25 mK to 300 K.

ENERGY CALCULATION BASED ON THE PROCESSED EXPERIMENTAL DATA

Infrared monitoring of the surface of examined specimen during quasistatic tension takes possibility to observe changes in temperature field in loading process. The Fig. 2 presents the stress strain relation and temperature evolution of the gage part of the specimen for investigated materials. We can divide the deformation process into three parts. At the beginning if the process the plastic deformation has a heterogeneous nature. We can observe the propagation of Luders bands (plastic deformation waves) on the specimen surface. This process is accompanied by the temperature wave propagation. The detail study of this part of plastic deformation in Armco iron can be found in [3].
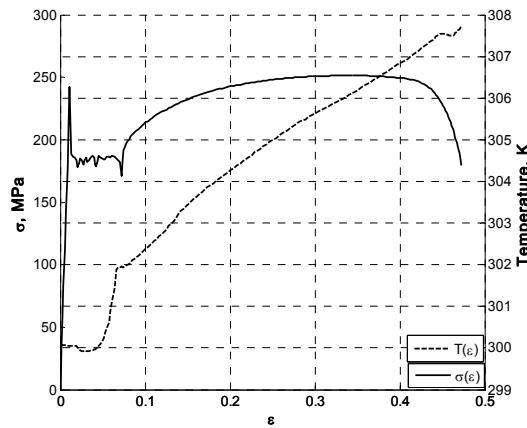
Figure 2: Stress – strain evolution of Armco iron specimen (solid line) and local temperature evolution (dash line); strain rate $2 \cdot 10^{-3}$ s^{-1}.

The plastic wave propagation is finished by the transition to hardening process accompanied by an approximately homogeneous plastic deformation of the sample (the second part of plastic deformation). The last part of the deformation process is characterized by necking heterogeneous temperature distribution of the specimen surface.

The second part of the process can be considered as a homogeneous at macroscopic level. The energy balance in specimen at this part of deformation will be simulated in the next part of this paper. All other parts of the process requests the consideration the nonlocal effects in defect ensemble and leads to the more complex model.

Heat sources calculation

The heat sources evolution can be calculated based on the following equation [4]

$$s(x, y, t) = \rho c \left(\frac{\partial T}{\partial t} + \frac{T}{\tau} \right) - k \left(\frac{\partial^2 T}{\partial x^2} + \frac{\partial^2 T}{\partial y^2} \right) \tag{1}$$

where

T is the temperature, ρ is the density (7870 kg/m³), c is the heat capacity (444 J/(kg·K)), k is the heat conductivity (76.2 W/(m·K)), s is the unknown specific power of heat source (W/m³) and τ is the constant describing the heat exchange process with the surroundings (160 sec) [5].

The definition of heat sources evolution requests the calculation of the space and time derivation of noisy temperature field. It leads to the situation when recorded experimental data of the temperature is not enough suitable to calculate the heat dissipation rate.

In this work we use time and space filter for experimental data. To implement filtration procedure it was applied discrete Fourier transform with Gaussian kernel. The peculiarities of filtering procedure are described in [6]. This procedure allows us to smooth spatial and time heterogeneity. Fig. 3 presents field of temperature range before and after processing.
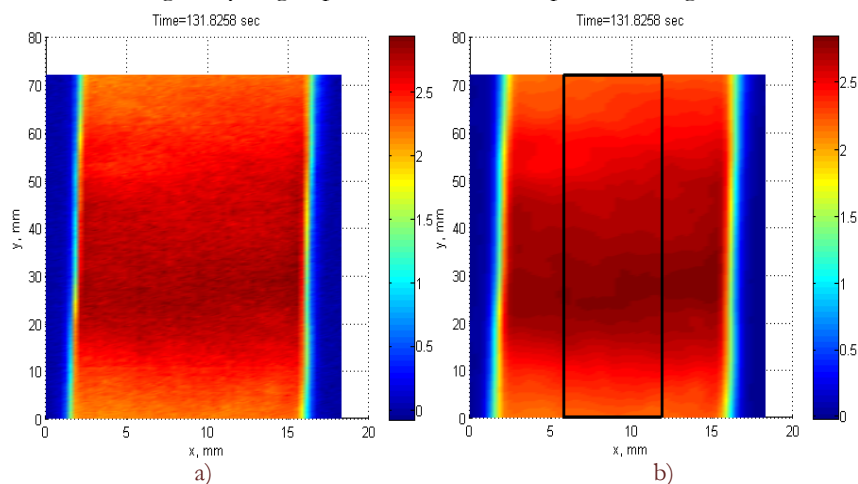

Figure 3: Temperature range on the surface of specimen before data processing (a) and obtained field of temperature range with zone of interest (b).

Stored energy calculation

Fig. 4 presents field of heat dissipation rate on the small area of specimen surface limited by black rectangle shown in Fig 3b. The small area for calculation was selected due to sample shape changing during deformation process. The field of heat sources is a little bit heterogeneous even during the second part of plastic deformation.
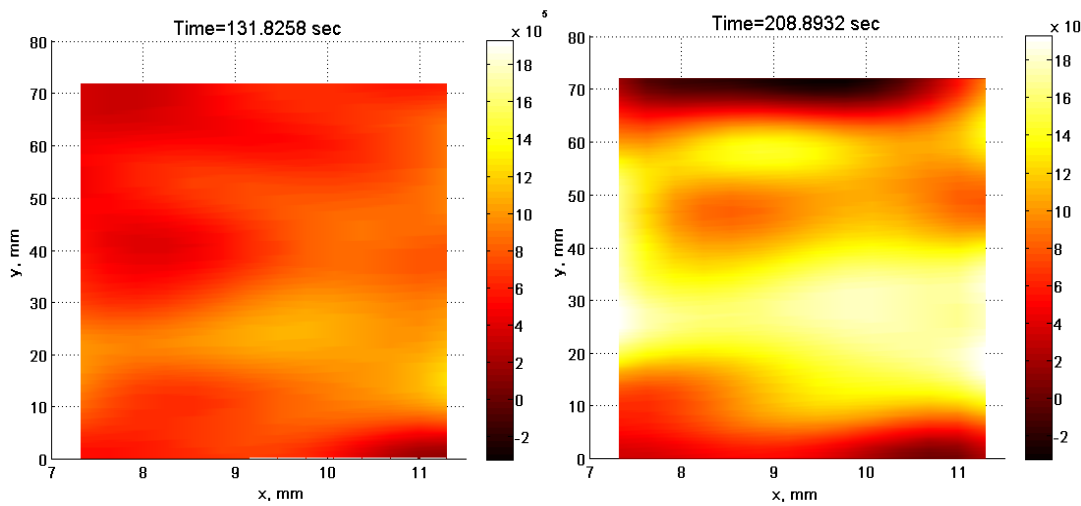

Figure 4: Experimental data of the heat dissipation rate (W/m³) at the beginning and end of interest time range.

The integral heat dissipation in zone of interest can be calculated as

$$Q(t) = \int\limits_{x_1}^{x_2} \int\limits_{y_1}^{y_2} s(x, y, t) dx dy \qquad (2)$$

where x_1, x_2, y_1, y_2 are the rectangular coordinates of the interest zone (Fig. 3b).

We suppose that some of the irreversible plastic work contributes to heat generation, while the rest is stored as the energy of crystal defects accompanying plastic deformation, traditionally known as the stored energy of cold work [7,8]. The goal of this work is to calculate value of the stored energy rate.

Plastic work spend on deformation of the specimen has to be known for calculation of the energy stored in metals during deformation. We obtained plastic work presented in expression (3) as a function of strain rate V and loading force $F(t)$.

$$W_p(t) = F(t)V \qquad (3)$$

We calculate stored energy of cold work as difference between plastic work spent on deformation and integral heat dissipation ($W_p(t) - Q(t)$) [9]. Time dependence of these values is shown in Fig. 5.

Ratio $\dfrac{Q(t)}{W_p(t)}$ is usually used for determination of the parameter β characterized extent of material damage [10]. The stored energy ratio can be calculated as follow

$$1 - \beta = \frac{W_p(t) - Q(t)}{W_p(t)} \qquad (4)$$

In Fig. 6 value of 1–β depending on strain is presented. Value of stored energy decreases in the end of deformation process that means most of plastic work converted into heat and materials prepared to the failure. Red line indicates part from 131.8 sec to 208.9 sec (surface of heat dissipation rate in the beginning and end of this range is presented in Fig.4) described the second part of plastic deformation. This part was chosen for numerical modeling of the plastic deformation process in Armco iron.
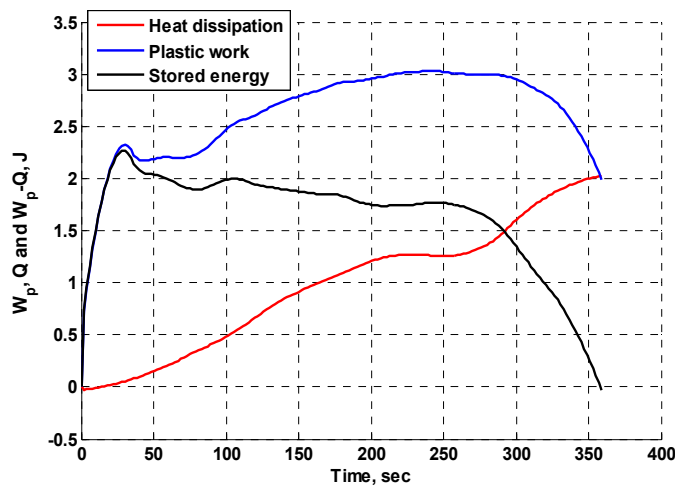
Figure 5: Time dependence of plastic work, heat dissipation energy and stored energy.
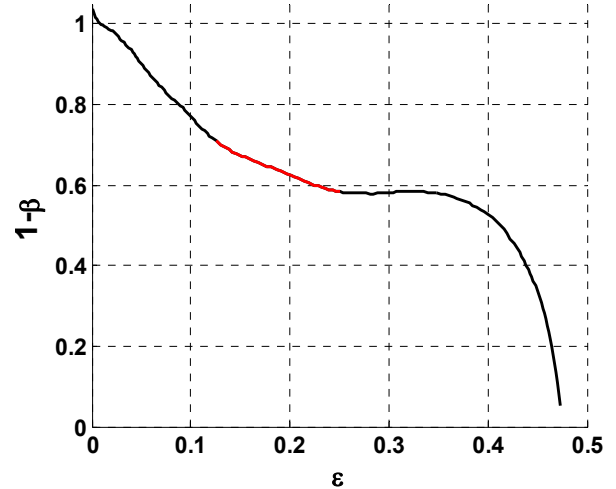
Figure 6: Strain dependences of stored energy ratio (1-β).

MATHEMATICAL MODEL OF ENERGY BALANCE IN METALS UNDER HOMOGENEOUS PLASTIC DEFORMATION

I t is now well known that real metals have complex structure, which is a hierarchy of different levels. Under deformation process the structural evolution observed at all scale levels and leads to irreversible deformation and destruction. To develop a model of defect evolution under plastic deformation we have to choose the basic physical level of description of the material microstructure and to describe the geometry of the elementary defects. One of the possible descriptions of defect kinetics is the statistical model of defect ensample. This model has to take into account the stochastically properties of defect initiation, their nonlinear integration and link between microplasticity and damage accumulation properties.

Problem statement

Typical mesoscopic defects (mesoshifts) are described as the symmetrical tensor $\tilde{s}$, which has the following form [11,12]:

$$\tilde{s} = \frac{1}{2} S'(\overline{n}\overline{l} + \overline{l}\overline{n})$$

where $\overline{l}$ is a unit normal to the shear plane, $\overline{b}$ is a unit vector in the shear direction, S' is a shift intensity.
Defect density tensor that coincides with the strain caused by defects is defined as:

$$\tilde{p} = n < \tilde{s} >$$

where n is a defect density.
The distribution function of defects can be represented in the following form:

$$W = Z^{-1} \exp(-E / \theta)$$

where E is the energy of the defect, Z is the normalizing factor, θ is the effective temperature factor responsible for the system susceptibility.
Averaging procedure lets us to obtain the self-consistency equation between micro and macro parameters in the following form:

$$\tilde{p} = N \int \tilde{s} W(\tilde{s}) d\tilde{s} \tag{5}$$

The solution of the Eq. (5) was proposed in [12]. Based on these results we can introduce a phenomenological model of the quasistatic process. Full strain rate can be represented as the sum of three components: elastic strain rate $\dot{\tilde{\varepsilon}}^e$, plastic strain rate $\dot{\tilde{\varepsilon}}^p$ and strain rate caused by defects $\dot{\tilde{p}}$:

$$\dot{\tilde{\varepsilon}} = \dot{\tilde{\varepsilon}}^e + \dot{\tilde{\varepsilon}}^p + \dot{\tilde{p}} \tag{6}$$

Elastic strains are defined by linear Hooke's law:

$$\dot{\sigma}_0 = K\dot{\varepsilon}_0^e \tag{7}$$

$$\dot{\tilde{\sigma}}_d = 2G\dot{\tilde{\varepsilon}}_d^{\,e} \tag{8}$$

where K - isotropic elastic modulus, G - elastic shear modulus, σ_0 - spherical part of the stress tensor, $\tilde{\sigma}_d$ - deviator part of the stress, ε^e_0 - spherical part of the elastic strain tensor, $\tilde{\varepsilon}_d^{\,e}$ - deviator part of the elastic strain.
Dissipation function for a medium with defects can be represented in the following form [13]:

$$\tilde{\sigma} : \dot{\tilde{\varepsilon}}^p + (\tilde{\sigma} - \rho\frac{\partial \Psi}{\partial \tilde{p}}) : \dot{\tilde{p}} - \overline{q} \cdot \frac{\nabla T}{T} \geq 0 \tag{9}$$

where Ψ is a free energy, ρ - density, $\overline{q}$ - heat flux vector, T - temperature.
Dividing the thermal and mechanical problems and basing on the Onsager principle, we can obtain from (9) constitutive equations for calculating kinetics of plastic and structural strains:

$$\dot{\tilde{\varepsilon}}^p = \Gamma_\sigma\tilde{\sigma} + \Gamma_{p\sigma}(\tilde{\sigma} - \rho\frac{\partial \Psi}{\partial \tilde{p}}) \tag{10}$$

$$\dot{\tilde{p}} = \Gamma_p(\tilde{\sigma} - \rho\frac{\partial \Psi}{\partial \tilde{p}}) + \Gamma_{p\sigma}\tilde{\sigma} \tag{11}$$

The kinetic coefficients Γ_σ, Γ_p and $\Gamma_{p\sigma}$ have the following form:

$$\Gamma_\sigma = \frac{1}{\tau_\sigma}\frac{1}{1 + Exp\left(-\dfrac{|\sigma| - S_c}{a_1}\right)}$$

$$\Gamma_p = \frac{1}{\tau_p}\frac{1}{1 + Exp\left(-\dfrac{H(|\sigma|,|p|,\delta,p_c,\sigma_c) - S_y}{a_2}\right)}$$

$$\Gamma_{p\sigma} = \frac{1}{\tau_{p\sigma}}$$

where τ_σ, τ_p, $\tau_{p\sigma}$ - characteristic relaxation times, $|\sigma|$ - stress intensity tensor, S_c a_1, a_2 - material constants, S_y - yield stress, $|p|$ - intensity of $\tilde{p}$, p_c, σ_c - scaling factors, $H(|\sigma|,|p|,\delta,p_c) = |\sigma| - 2\mu\sigma_c\left[\delta(f+1)|p|p_c - |p|p_c\right]$ - material function (it can be considered as "degree of system nonequilibrium").
It is supposed that thermodynamic force $\tilde{\sigma} - \rho\dfrac{\partial \Psi}{\partial \tilde{p}}$ can be written as:

$$\tilde{\sigma} - \frac{\partial \Psi}{\partial \tilde{p}} = \left[\frac{1}{\delta}\left(\frac{\tilde{\sigma}}{2G\sigma_c} + \frac{\tilde{p}}{p_c}\right) - \left(f\left(\frac{|p|}{p_c}\right)\frac{p_c}{|p|} + 1\right)\frac{\tilde{p}}{p_c}\right] \tag{12}$$

where $f(|p|)$ denotes a power function for modeling of nonlinear hardening process:

$$f\left(\frac{|p|}{p_c}\right) = k\left(\frac{|p|}{p_c}\right)^a \tag{13}$$

k is a scaling factor, a is the exponent.
Eqs. (6)-(8) and (10)-(13) represent a closed system for a plastically deformed solid with nonlinear hardening.
From the first thermodynamic law, we can obtain the expression for calculation the β parameter in the following form:

$$\beta = \frac{\dot{Q}^p}{\dot{W}^p} = 1 - \frac{\left[\rho\dfrac{\partial\Psi}{\partial\tilde{p}} - \rho T\dfrac{\partial^2\Psi}{\partial T\partial\tilde{p}}\right]:\dot{\tilde{p}}}{\tilde{\sigma}:(\dot{\tilde{\varepsilon}}^p + \dot{\tilde{p}})}$$

where Q^p - inelastic contribution to the heat, W^p - plastic work. Under isoentropy conditions it has the form:

$$\beta = \frac{\dot{Q}^p}{\dot{W}^p} = 1 - \frac{\rho\dfrac{\partial\Psi}{\partial\tilde{p}}:\dot{\tilde{p}}}{\tilde{\sigma}:(\dot{\tilde{\varepsilon}}^p + \dot{\tilde{p}})}$$

Results of modeling

Fig. 7 presents the experimental results for tension of Armco iron samples. To simulate the homogeneous part of plastic deformation, we propose the existence of two process steps. The first step is corresponding to the loading of the sample up to yield stress, Luders bunds propagation and unloading. The second step corresponds to the loading of preloaded specimen. During the second step the specimen exhibits the homogeneous plastic deformation, parabolic hardening and decreasing of stored energy ratio. This process can be simulated by definition of nonzero initial deformation. The schematic of the process is presented in Fig. 7.
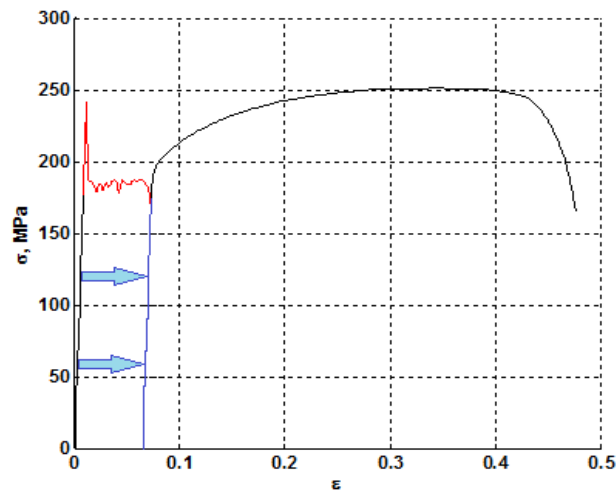

Figure 7: Experimental stress-strain curve for Armco iron.

Numerical simulation of the considered process was carried out in the finite element package Simulia Abaqus 6.13. Fig. 8 shows the finite-element mesh of the specimen. Eight-node linear brick elements were used for the simulation. The above explained model was applied for the material behavior description using the subroutine UMAT. Arrays of material constants, strain, strain increments and the time step passed as input data to the procedure. Increments of the stress tensor components and increments of the defect density tensor components are determined from the system of constitutive equations. Values of these components at the next time step are defined as the sum of the values on the previous step and the appropriate increment.

Fig. 9 presents the stress-strain curves obtained from experimental data (dash dot line) and results of numerical simulation (solid line). Results calculated by the model are in a good agreement with experiment.
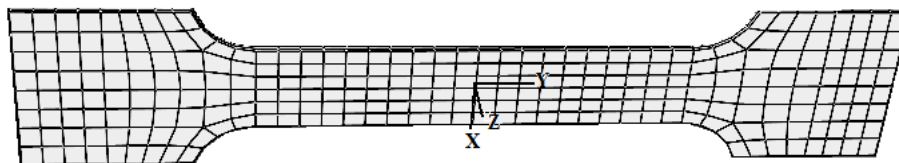

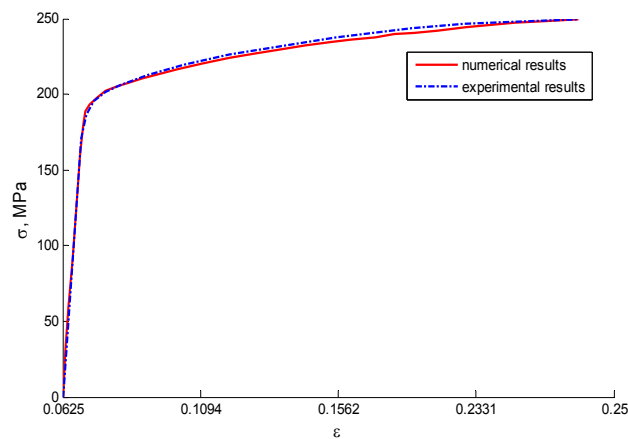Figure 8: Finite-element mesh of the specimen.

Figure 9: Numerical and experimental stress-strain curves for Armco iron.

Fig. 10 demonstrates the simulation results of the 1–β value. The modeling results coincide to the experimental on the homogeneous stage of the plastic deformation. Dash line corresponds to the red line in Fig. 6.

The numerical results exhibit increasing branch of stored energy ratio and coincide to the experimental results after some deformation value. This fact can be explained by the initial conditions for structural sensitive parameters of the model defined in the simulation process. The initial condition corresponds to the annealed materials with zero defect induced deformation. At the beginning of deformation process this material exhibits increasing rate of stored energy ratio corresponding to the increasing of defect density [1]. In contrast to this, the experimental result corresponds to initially deformed material which has created effective defect structure for the dissipation of deformation energy. The extension of the area of applicability of the model requests the simulation of nonlocal process of plastic deformation.
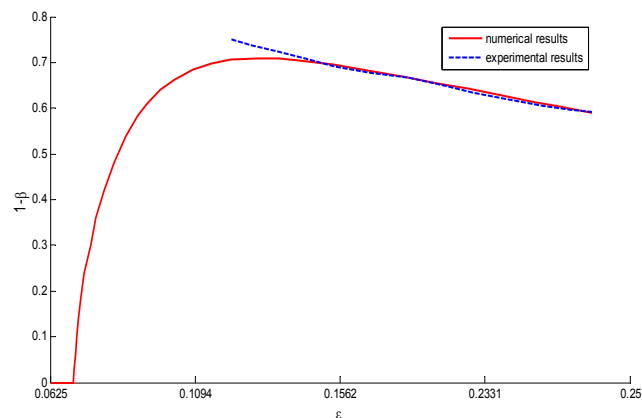

Figure 10: Value of 1-β depending on strain. Simulation results.

CONCLUSION

The infrared technique has been applied to investigate the effect of heat dissipation under quasistatic loading of Armco iron. A technique for experimental data treatment has been developed for determination of the stored energy rate. The heat dissipation field and average stored energy ration were calculated for whole deformation process including homogeneous and heterogeneous pats.

The experimental results stimulate us to develop a phenomenological model describing the energy balance in metals under plastic deformation. Extending the previous results of the research group in Perm, we propose a statistical description of the mesodefect ensemble and introduce the thermodynamic potential of solid with defect. The key point of the model is definition of defect induced strain which can be considered as a thermodynamic variable. It allowed us to propose a three dimensional thermodynamic internal variable model of heat dissipation in metals and describe the energy storage in Armco iron under homogeneous plastic deformation.

The calculated value of stored energy rate was compared with experimentally determined value. A good agreement between experimental and numerical results in the range of homogeneous plastic deformation was found.

NOMENCLATURE

$\bar{b}$	unit vector in the shear direction
c	heat capacity
E	defect energy
F	loading force
G	elastic shear modulus
IR	infrared
k	heat conductivity
K	isotropic elastic modulus
$\bar{l}$	unit normal vector to the shear plane
n	defect density
$\tilde{p}$	mesoscopic defect density tensor
$|p|$	intensity of $\tilde{p}$
$\bar{q}$	heat flux vector
Q	specific energy dissipation rate integrated over the coordinates
Q^p	inelastic contribution to the heat
$\tilde{s}$	microscopic defect tensor
S	specific energy dissipation rate
S'	shift intensity
S_y	yield stress
T	temperature
V	strain rate
W	distribution function of defects
W_p	plastic work
Z	normalizing factor
β	variable characterized extent of material damage
$\tilde{\varepsilon}^e$	elastic strain tensor
ε^e_0	spherical part of the elastic strain tensor
$\tilde{\varepsilon}^e_d$	deviator part of the elastic strain
$\tilde{\varepsilon}^p$	plastic strain tensor
ϱ	density
$\tilde{\sigma}$	Cauchy stress tensor
$|\sigma|$	stress intensity tensor
σ_0	spherical part of the stress tensor

$\tilde{\sigma}_d$	deviator part of the stress tensor
τ_i, $i = p, p\sigma, \sigma$	characteristic relaxation times
τ	the constant describing the heat exchange process with the surroundings
Ψ	free energy

REFERENCES

[1] Bever, M.B., Holt, D.L., Tichener, A.L., The stored energy of cold work, Progress in Materials Science, 17 (1973) 5–173.

[2] Fedorova, A.Yu., Bannikov, M.V., Plekhov, O.A., A study of the stored energy in titanium under deformation and failure using infrared data, Fracture and Structural Integrity, 24 (2013) 81-88.

[3] Plekhov, O.A., Naimark, O.B., Saintier, N., Palin-Luc, T., Elastic-plastic transition in iron: Structural and thermodynamic features, Technical Physics, 54(8) (2009) 1141-1146.

[4] Chrysochoos, A., Louche, H., An infrared image processing to analyse the calorific effects accompanying strain localization, International Journal of Engineering Science, 38 (2000) 1759–1788.

[5] Chrysochoos, A., Balandraud, X., Wattrisse, B., Identification procedure using full-field measurements applications in mechanics and structures, Processing of CNRS summer school, 2013 May 21-25; Montpellier, France.

[6] Fedorova, A.Yu., Bannikov, M.V., Plekhov, O.A., Infrared thermography study of the fatigue crack propagation, Fracture and Structural Integrity, 21 (2012) 46-53.

[7] Hodowany, J., Ravichandran, G., Rosakis, A.J., Rosakis, P., Partition of plastic work into heat and stored energy in metals, Exp. Mech., 40(2) (2000) 113–123.

[8] Plekhov, O., Uvarov, S., Naimark, O., Theoretical and experimental investigation of dissipated and stored energy ratio in iron under quasi-static and cyclic loading, Strength of materials, 1(391) (2008) 101–105.

[9] Taylor, G.I., Quinney, H., The latent energy remaining in a metal after cold working, Proc. R. Soc. A, 143 (1934) 307–326.

[10] Rittel, D., Wang, Z.G., Merzer, M., Adiabatic shear failure and dynamic stored energy of cold work, Physical Review Letters, 96 (2006) 075502(1–4).

[11] Naimark, O.B., Structural-scaling transitions in mesodefect ensembles as mechanisms of relaxation and failure in shocked and dynamically loaded materials (experimental and theoretical study), J. Phys. IV. France, 134 (2008) 3–9.

[12] Naimark, O.B., Bayandin, Yu.V., Leontiev, V.A., Panteleev, I.A., Plekhov, O.A., Structural-scaling transitions and thermodynamic and kinetic effects in submicro-(nano)crystalline bulk materials, Phys. Mesomech., 12(5-6) (2009) 239–248.